Quantum dynamics through conical intersections in macrosystems: Combining effective modes and time-dependent Hartree

ARTICLE *in* CHEMICAL PHYSICS · MAY 2008

Impact Factor: 1.65 · DOI: 10.1016/j.chemphys.2007.09.047

4 AUTHORS, INCLUDING:

Mathias Basler
Universität Heidelberg
2 PUBLICATIONS **11** CITATIONS
SEE PROFILE

Etienne Gindensperger
CNRS - University of Strasbourg
29 PUBLICATIONS **546** CITATIONS
SEE PROFILE

Hans-Dieter Meyer
Universität Heidelberg
245 PUBLICATIONS **9,841** CITATIONS
SEE PROFILE

Available online at www.sciencedirect.com
ScienceDirect
Chemical Physics 347 (2008) 78–96
Chemical Physics
www.elsevier.com/locate/chemphys

Quantum dynamics through conical intersections in macrosystems: Combining effective modes and time-dependent Hartree

Mathias Basler, Etienne Gindensperger *, Hans-Dieter Meyer, Lorenz S. Cederbaum

Theoretische Chemie, Universität Heidelberg, Im Neuenheimer Feld 229, D-69120 Heidelberg, Germany

Received 1 August 2007; accepted 15 September 2007
Available online 4 October 2007

It is a pleasure for us to dedicate this work to Professor Wolfgang Domcke on the occasion of his 60th birthday.

Abstract

We address the nonadiabatic quantum dynamics of (macro)systems involving a vast number of nuclear degrees of freedom (modes) in the presence of conical intersections. The macrosystem is first decomposed into a system part carrying a few, strongly coupled modes, and an environment, comprising the remaining modes. By successively transforming the modes of the environment, a hierarchy of effective Hamiltonians for the environment can be constructed. Each effective Hamiltonian depends on a reduced number of effective modes, which carry cumulative effects. The environment is described by a few effective modes augmented by a residual environment. In practice, the effective modes can be added to the system's modes and the quantum dynamics of the entire macrosystem can be accurately calculated on a limited time-interval. For longer times, however, the residual environment plays a role. We investigate the possibility to treat fully quantum mechanically the system plus a few effective environmental modes, augmented by the dynamics of the residual environment treated by the time-dependent Hartree (TDH) approximation. While the TDH approximation is known to fail to correctly reproduce the dynamics in the presence of conical intersections, it is shown that its use on top of the effective-mode formalism leads to much better results. Two numerical examples are presented and discussed; one of them is known to be a critical case for the TDH approximation.

Keywords: Nonadiabatic quantum dynamics; Conical intersection; Effective modes; MCTDH; System–environment splitting

1. Introduction

Conical intersections (CIs), once considered as highly pathological, are nowadays recognized as a paradigm for ultrafast nonadiabatic processes occurring in molecular systems [1–9]. They correspond to particular topologies of intersecting electronic potential-energy surfaces, signaling a complete breakdown of the Born–Oppenheimer approximation. The electronic and nuclear motions then strongly couples, and CIs act as photochemical funnels which allow for ultrafast electronic relaxations, typically on a femtosecond time-scale. CIs are found, for instance, in nucleobases such as Adenine [10], in the retinal chromophore [11], etc. A large collection of examples involving CIs and references to a wide selection of articles on the subject can be found in Ref. [8].

The abundance of CIs grows with the dimensionality of the problem [12], *i.e.*, with the number of nuclear degrees of freedom (vibrational modes). While already present in small molecular species, CIs become more and more common in larger and larger systems. By allowing for ultrafast nonadiabatic electronic transitions, CIs are by essence of quantum nature. This manifests itself, among other, by geometric phase effects [13]. Another key-feature of

* Corresponding author. Present address: Institut de Chimie, Laboratoire de Chimie Quantique, UMR 7177 CNRS / Université Louis Pasteur, 4 rue Blaise Pascal, 67000 Strasbourg, France.
E-mail address: etienne.gindensperger@chimie.u-strasbg.fr (E. Gindensperger).

0301-0104/$ - see front matter © 2007 Elsevier B.V. All rights reserved.
doi:10.1016/j.chemphys.2007.09.047

CI-topologies is their important sensibility to all the parameters of the problem. When the molecular system comprises a vast number of vibrational modes, what we shall call a "macrosystem" in the following, all the modes may play an important role. Usually, in such cases, the macrosystem is decomposed into a system part and an environment. When we are dealing with molecular species embedded in a (true) environment, this separation is obvious. We may think, e.g., of a chromophore in a protein pocket or an impurity in a crystal. In many other situations, for instance when studying a large isolated molecule, it is also useful to allow for a system/environment splitting. Here, typically, the system is comprised of the strongest coupled modes which are supposed to dominate the dynamics. The vast number of remaining modes are then collected in an environment.

If a given environmental mode may individually have a small impact, the vast collection of modes leads to cumulative effects which are typically large in CI situations [14–18]. One of the issue, in this context, is to be able to obtain a realistic description of the macrosystem's dynamics. This implies, in principle, a quantum treatment of all the degrees of freedom: those of the system and those of the environment. Currently, the multiconfiguration time-dependant Hartree (MCTDH) method [19–22], one of the best method available to date, is able to treat the dynamics of 20–30 modes in the presence of CIs [15,23–28]. This number can be increased using the multi-layer extension of MCTDH [22,29,30]. For a truly large number of modes, an explicit, numerically exact treatment of all the vibrational modes becomes difficult to achieve. Then, one can resort to approximate dynamical methods, see, for instance Refs. [31,32], or may use strategies related to dissipation theory, see, e.g., Ref. [16].

Another strategy is to construct reduced models: the vast number of environmental modes are represented by a few collective or effective modes only. The drastically reduced number of modes thus allows for a numerically exact treatment of the dynamics. The main question is then: how can we construct such effective modes, and how do they perform in subsuming a truly large environment.

This question has been addressed recently [18]. There, it has been shown that the use of *three effective environmental modes* only – together with the system's modes – suffice to calculate accurately the band shape and short-time dynamics of the entire macrosystem. Detailed analysis of the effective-mode formalism along with numerical applications can be found in Refs. [33–36]. Precursors of this approach were derived more than 20 years ago for the Jahn–Teller effect [37–42]. This approach allows to split the environment into two parts: (i) a primary set of three effective modes which couples to the system's modes and carry the environmental effect on a short-time-scale, and (ii) a "residual environment" which couples only to the effective modes and becomes important at later times.

If time-scales beyond short times are under interest, the use of these three effective modes is, however, not sufficient, and one has to take into account the residual environment. This can be done by constructing additional sets of effective modes, as recently proposed in Ref. [43]. Indeed, it has been shown analytically that the systematic use of additional effective modes allows to calculate accurately the quantum dynamics for longer and longer times [44]. In this vein, a related extension of the effective-mode theory has been used to analyze exciton dissociation in semiconducting polymers [45–47].

The environment is thus described by more and more effective modes as the time increases [43,44]. However, even with MCTDH, we can deal only with a limited number modes in total: this number will correspond to the system's modes augmented by some effective modes. This will provide an accurate description of the dynamics on a limited time-interval. If one still needs to describe the dynamics on a longer time-scale, one has to use an approximate dynamical treatment for the residual modes.

In this paper, we want to investigate the combination of the effective-mode formalism with the additional, approximate treatment of the residual environment: the dynamics of the system plus some effective modes is treated numerically exactly, with MCTDH, and only the dynamics of the residual environment is approximate. We choose as approximation the time-dependent Hartree (TDH) method [48,49]. This approximation has the advantage of a very small numerical requirement, scaling only linearly with the number of residual modes, which renders its use practicable for truly large environments. Furthermore, its implementation within MCTDH is straightforward. However, TDH neglects all the correlation between the modes, and is known to fail to reproduce correctly the dynamics of an environment in CI situations [50]. We investigate in this paper how this simple approximation, used *on top* of the effective-mode formalism, performs.

The paper is organized as follows. In Section 2 we briefly discuss the effective-mode formalism as well as the MCTDH method, and its combination with the TDH approximation. In Section 3 we present two numerical examples to illustrate how the effective modes perform and what does the additional treatment of the residual environment by TDH. For the first example, we use one of the model system–environment complexes presented in Ref. [35], which corresponds to a general case of the effective-mode formalism. The second example exploits the model environment proposed by Krempl et al. [51] to study the pyrazine molecule, and corresponds to a particular case of the formalism. Section 4 concludes.

2. Theory and method

2.1. The effective-mode formalism

In this section, we introduce the effective-mode formalism which is the cornerstone of the present study. This formalism consists of the systematic construction of sets of effective modes to describe the dynamics of electronically

excited macrosystems. The construction of effective modes relies on successive orthonormal transformations (rotations) of the vibrational modes which describe the Hamiltonian of the macrosystem. Below, we present the Hamiltonian of the macrosystem used in this work, and expose the subsequent construction of the sets of effective modes.

2.1.1. The Hamiltonian of the macrosystem

The Hamiltonian of the macrosystem is written as a "system part" interacting with an "environment" in a diabatic representation as follows:

$$H = H_S + H_B \tag{1}$$

with the system's Hamiltonian comprised of N_S modes

$$H_S = \begin{pmatrix} E_1 + T_S + V_{11} & V_{12} \\ V_{21} & E_2 + T_S + V_{22} \end{pmatrix} \tag{2}$$

and the Hamiltonian of the environment with N_B modes

$$H_B = \sum_{i=1}^{N_B} \frac{\omega_i}{2}(p_i^2 + x_i^2)\mathbf{1} + \begin{pmatrix} \sum_{i=1}^{N_B} \kappa_i^{(1)} x_i & \sum_{i=1}^{N_B} \lambda_i x_i \\ \sum_{i=1}^{N_B} \lambda_i x_i & \sum_{i=1}^{N_B} \kappa_i^{(2)} x_i \end{pmatrix}. \tag{3}$$

H_S and H_B interact since they do not commute – the interaction between the vibrational modes is mediated by the electronic subsystem. In Eq. (2), E_1 and E_2 are constants ($E_1 < E_2$) representing the energy of the electronic states at the reference geometry, T_S is the system's kinetic energy operator and the $V_{ij}(\{x_S\})$ are the diabatic potential-energy operators for the ensemble $\{x_S\}$ of the N_S modes of the system. The Hamiltonian (2) describes two coupled electronic states and generates a conical intersection within the system. We do not specify the exact form of the potentials, since their particular structure is not essential for the discussion. We suppose throughout this paper that the dynamics provided by the system's Hamiltonian can be calculated numerically, *i.e.*, N_S is not too large.

H_B, Eq. (3), governs the nuclear motion of the N_B modes of the environment with frequencies ω_i, mass- and frequency-scaled dimensionless coordinates x_i and canonical momenta p_i. $\mathbf{1}$ is the unit matrix and the quantities $\kappa_i^{(1)}$, $\kappa_i^{(2)}$ and λ_i denote the so-called intrastate and interstate coupling constants, respectively.

The Hamiltonian of the environment, H_B, is described by the linear vibronic coupling (LVC) model [1,8,9]. This model Hamiltonian reproduces correctly the adiabatic potential-energy surfaces in the vicinity of the conical intersection. The LVC model is accurate near the CI, but becomes less accurate further away from the CI, if quadratic and higher-order terms (e.g., anharmonicity of the diabatic surfaces) cannot be neglected. We note, however, that not all modes of the macrosystem need to be treated as being part of the environment: the most anharmonic or strongest coupled modes could be included in the system which is not restricted to any kind of model in the present study. Hence, as usual, the separation of the macrosystem into system and environment is somewhat arbitrary and a matter of convenience. The dynamics induced by a conical intersection is typically fast and to describe such a dynamics the use of the LVC ansatz for the great majority of the modes (the others are to be included in the system) is sufficient. In general, it is the large number of environmental modes which precludes the computation of the full, numerically exact quantum dynamics of the entire macrosystem.

2.1.2. Hierarchy of effective Hamiltonians for the environment

In the LVC Hamiltonian H_B, all the environmental modes play formally the same role: they can tune and/or couple the electronic states. Importantly, in truly large macrosystems, even weakly coupled modes can play a crucial role since their vast number can lead to cumulative effects which can be large. In such cases, to include a few environmental modes only and to neglect the majority of the environment cannot, in general, be sufficient to describe properly the impact of the latter onto the system. Interestingly, however, the cumulative effects of the environment on the system's dynamics can be taken into account by employing a limited number of *effective modes*. This is the underlying idea of the effective-mode formalism [18] where the use of a reduced number of effective modes to represent the environment allows to simulate the dynamics of the entire macrosystem accurately on a short-time-scale.

In the following, various sets of effective modes will be constructed. Each set span what we shall call an effective Hamiltonian and the series of these effective Hamiltonians constitutes a hierarchy. Following Ref. [43], the Hamiltonian of the environment, H_B of Eq. (3), can be *exactly* re-written as

$$H_B = H_1 + H_{r1}, \tag{4}$$

$$= H_1 + H_2 + H_{r2}, \tag{5}$$

$$\vdots$$

$$H_B = \sum_{m=1}^{n} H_m + H_{rn} \tag{6}$$

with H_m being the mth member of the hierarchy of effective Hamiltonians, and H_{rm} the corresponding *residual environment*. For the 2-state conical-intersection situations, which is in the focus of this work, each effective Hamiltonian is comprised of a maximum number of three effective modes only [18,33,34]. The remaining environmental modes enter in the corresponding residual Hamiltonian.

The first member of the hierarchy, H_1, and its residual environment H_{r1}, were first derived in Ref. [18] and details about their construction can be found in Ref. [33]. Let us briefly sketch how they are constructed starting from the original Hamiltonian of the environment. Examining the original Hamiltonian of the environment, Eq. (3), we readily see that we can identify three effective modes given by $\sum_{i=1}^{N_B} \kappa_i^{(1)} x_i$, $\sum_{i=1}^{N_B} \kappa_i^{(2)} x_i$ and $\sum_{i=1}^{N_B} \lambda_i x_i$. These three effective

modes suffices to describe the second term of H_B in Eq. (3), *i.e.*, the part of H_B which couples the electronic states. These three effective modes are however not orthogonal to each other. By an appropriate orthonormalization of these modes, and by the construction of $N_B - 3$ additional modes orthonormal to the first three effective modes and among themselves, we construct a full, N_B-dimensional transformation matrix $\boldsymbol{T}$ from the vector of the original modes $\mathbf{x} = \{x_i\}$ to the vector of the new modes $\boldsymbol{X} = \{X_i\}$, $i = 1, \ldots, N_B$: $\boldsymbol{X} = \boldsymbol{T}\boldsymbol{x}$. Inserting this transformation in the original Hamiltonian H_B of Eq. (3), we obtain the new form $H_1 + H_{r1}$ of Eq. (4), where H_1, the first effective Hamiltonian, is described by three effective modes only and is given by [18,33]:

$$H_1 = \sum_{i=1}^{3} \frac{\Omega_i}{2}(P_i^2 + X_i^2)\mathbf{1} + \begin{pmatrix} \bar{\kappa}^{(1)} \sum_{i=1}^{3} K_i^{(1)} X_i & \bar{\lambda} \sum_{i=1}^{3} \Lambda_i X_i \\ \bar{\lambda} \sum_{i=1}^{3} \Lambda_i X_i & \bar{\kappa}^{(2)} \sum_{i=1}^{3} K_i^{(2)} X_i \end{pmatrix}, \tag{7}$$

where

$$\bar{\kappa}^{(\alpha)} = \left[\sum_{i=1}^{N_B} (\kappa_i^{(\alpha)})^2\right]^{1/2}, \quad \alpha = 1, 2; \quad \bar{\lambda} = \left[\sum_{i=1}^{N_B} (\lambda_i)^2\right]^{1/2} \tag{8}$$

are effective coupling constants. The quantities $K_i^{(\alpha)} = \sum_j \kappa_j^{(\alpha)} t_{ij}/\bar{\kappa}^{(\alpha)}$ and $\Lambda_i = \sum_j \lambda_j t_{ij}/\bar{\lambda}$, $i = 1, 2, 3$, with t_{ij} the elements of $\boldsymbol{T}$, are normalization constants representing how the effective couplings are distributed among the three effective modes. The residual environment H_{r1} contains the $N_B - 3$ remaining environmental modes and reads

$$H_{r1} = \sum_{i=4}^{N_B} \frac{\Omega_i}{2}(P_i^2 + X_i^2)\mathbf{1} + \sum_{i=1}^{3} \sum_{j=4}^{N_B} d_{ij}(P_i P_j + X_i X_j)\mathbf{1}. \tag{9}$$

The frequencies Ω_i and coupling constants d_{ij} are obtained from the initial frequencies ω_i and the elements of the transformation matrix [33]:

$$\Omega_i = \sum_{k=1}^{N_B} \omega_k t_{ik}^2, \quad d_{ij} = \sum_{k=1}^{N_B} \omega_k t_{ik} t_{jk}. \tag{10}$$

The first member of the hierarchy of effective Hamiltonians, H_1 of Eq. (7), contains two terms. The first term consists of harmonic oscillators, and the second couples the electronic states. This second term is characterized by the effective coupling constants (bar quantities of Eq. (8)), which carry cumulative effects of all the N_B modes of the original environment. The residual environment H_{r1} given by Eq. (9) is described by $N_B - 3$ remaining modes, and also contains two terms. The first one consists of harmonic oscillators, and the second one is made of bilinear potential and kinetic couplings between the three effective modes of H_1 and the remaining modes. Importantly, H_{r1} is diagonal in the electronic space. Consequently, all the coupling between the two electronic states due to the environment is contained in H_1 only; the residual environment H_{r1} do not contribute to the coupling of the electronic states.

We already see a striking difference between the original H_B and its first transformed version $H_1 + H_{r1}$: for the latter, only *three* effective modes participate directly to the coupling of the electronic states, while in the original Hamiltonian of the environment *all* modes may do so. As a consequence, the remaining modes of H_{r1} do not couple directly to the system's modes of H_S, this coupling is only indirect and mediated by H_1. The implications of this property regarding, for instance, the topology near the conical intersection, have been discussed [34,33]. Importantly, it has been shown that the use of H_1 alone to represent the environment, *i.e.*, the complete neglect of all the $N_B - 3$ modes of H_{r1}, suffices to reproduce accurately the short-time dynamics of the entire macrosystem [18,33]. This property will be discussed later in more details (Section 2.1.3). Various numerical examples substituting the three-mode Hamiltonian H_1 to the N_B-mode Hamiltonian H_B are presented and discussed in Refs. [18,34,36,35].

When time-scales beyond short times are of interest, the remaining environment must be accounted for to obtain an accurate description of the dynamics. An explicit account of all the $N_B - 3$ remaining modes is however not feasible in a numerically exact treatment. One can, nevertheless, construct additional effective modes out of the remaining environment, in a similar way as done for the original environment. This idea has been used to build a hierarchy of effective Hamiltonians [43] and is exposed in the following. We also refer to the work of Tamura et al. who use a similar approach for the study of exciton dissociation in semiconducting polymers [45–47].

The construction of the higher members of the hierarchy of effective Hamiltonians is done in an analogous way than the construction of the first member. To construct the second member of the hierarchy H_2, we identify three additional effective modes in the first residual environment H_{r1} [43]. Examining Eq. (9), we identify the three modes in question: $\sum_{j=4}^{N_B} d_{ij} X_j$, for $i = 1, 2, 3$, where the index i refers to the first three effective modes which span the first effective Hamiltonian H_1 and j refers to the $N_B - 3$ modes of H_{r1}. These three non-orthogonal additional modes are then properly orthonormalized and augmented by $N_B - 6$ additional orthonormal modes to obtain a transformation matrix in the $N_B - 3$-dimensional space of the modes of H_{r1}. The residual environment H_{r1} is transformed accordingly and becomes $H_2 + H_{r2}$. As we shall see, the mathematical form of H_{r2} is similar to that of H_{r1}. Consequently, H_{r2} can be transformed as well in a completely analogous way into $H_3 + H_{r3}$. And so on, the member H_m of the hierarchy is constructed from the former residual environment H_{rm-1} and reads for $m > 1$ [43]

$$H_m = \sum_{i=3(m-1)+1}^{3m} \frac{\Omega_i}{2}(P_i^2 + X_i^2)\mathbf{1} + \sum_{i=3(m-2)+1}^{3(m-1)} \sum_{j=3(m-1)+1}^{3m} d_{ij}(P_i P_j + X_i X_j)\mathbf{1}. \tag{11}$$

The mth residual environment is given by

$$H_{rm} = \sum_{i=3m+1}^{N_B} \frac{\Omega_i}{2}(P_i^2 + X_i^2)\mathbf{1} + \sum_{i=3(m-1)+1}^{3m} \sum_{j=3m+1}^{N_B} d_{ij}(P_iP_j + X_iX_j)\mathbf{1}. \quad (12)$$

Except of H_1, all members of the hierarchy of effective Hamiltonians have the same mathematical form. The corresponding remaining environments have also the same form, only the number of modes varies. It is to be noted that each time a new member of the hierarchy is constructed, the modes of the residual environment out of which the new member is build are rotated and thus change as well as the frequencies Ω_i and the couplings d_{ij}. However, we keep the same notation for these quantities for simplicity. For details regarding the specific choices of the orthonormal transformations of the modes see Ref. [43].

Being constructed from the residual environment H_{r1}, all the members of the hierarchy H_m with $m > 1$, Eq. (11), are diagonal in the electronic space. Each one of these effective Hamiltonians is described by three effective modes, and contains two terms. The first one is comprised of the harmonic-oscillator contributions, and the second one contains bilinear kinetic and potential couplings between the effective modes of the mth member and those of the former member $m-1$. Regarding the residual environments, H_m of Eq. (12), they are all of the same mathematical form as H_{r1} but contains less and less modes as m increases. They couple only to the last member of the hierarchy, *i.e.*, H_{rm} couples only to H_m and not (directly) to the other members of the hierarchy H_k with $k < m$. The residual environment contains obviously all the modes which are not included in the effective Hamiltonians belonging to the hierarchy. For instance, if we construct two effective Hamiltonians, each of these Hamiltonians contains three effective modes and H_{r2} the rest, *i.e.*, $N_B - 6$ modes. Note that the successive transformations of H_B are all orthogonal, and thus preserves the physics provided by the original LVC Hamiltonian. And, since the system part H_S is not involved in these transformations, the properties of the Hamiltonian of the entire macrosystem are preserved as well.

A direct consequence of the construction of the hierarchy of effective Hamiltonians is the construction of a *sequential coupling of effective modes* [43]. Only the first set of effective modes spanning H_1 couples directly (via the electronic subsystem) to the system's modes; the effective modes of the second member of the hierarchy couples to the modes of the first member; the third member couples to the second, etc. And finally, the residual environment couples only to the last member of the hierarchy. Of course, the construction of the hierarchy can be pursued until the original Hamiltonian has been fully transformed in a complete hierarchy; then, no more residual environment subsists.

To include all the N_B modes of the environment in a numerically exact calculation of the quantum dynamics is out of reach even when using the transformed Hamiltonian of Eq. (6). However, the hierarchy, with its particular form leading to a sequential coupling of the effective modes, is particularly appropriate for approximations. This is highlighted by considering a fundamental dynamical property of the effective-mode formalism in what follows.

2.1.3. Dynamical property of the effective-mode formalism

There is a strong link between the sequential coupling of the members of the hierarchy of effective Hamiltonians and the dynamical properties of the entire macrosystem. Indeed, it has been shown that the use of a few members of the hierarchy of effective Hamiltonians, along with the system's modes, suffices to reproduce accurately the dynamics of the entire macrosystem on a given time-scale [18,33–36,43–46]. This is related to a moment expansion of the autocorrelation function as explained in the following. The autocorrelation function $C(t)$ measures the overlap between the initial wavepacket $|\Psi(0)\rangle$ and the one which evolves in time on the coupled electronic states $|\Psi(t)\rangle$:

$$C(t) = \langle\Psi(0)|\Psi(t)\rangle = \langle\Psi(0)|e^{-iHt}|\Psi(0)\rangle \quad (13)$$

with $\hbar = 1$. Here, the initial wavepacket have two components $\tau_1|0\rangle$ and $\tau_2|0\rangle$, one for each electronic state. τ_i corresponds to the transition dipole moment or ionization cross-section for the state i, depending on the problem under interest, and $|0\rangle$ is the vibrational wavepacket of the initial, usually ground electronic state of the macrosystem. We suppose that this initial vibrational wavepacket can be written as a direct product of the system's vibrational wavefunction and that of the environment. The latter is described by a direct product of Gaussian, corresponding to the vibrational ground-state of the Hamiltonian of the environment.

Expanding the autocorrelation function as a Taylor series in time, one obtains [52]

$$C(t) = \sum_{k=0}^{\infty} \frac{(-it)^k}{k!} M_k \quad (14)$$

with the moments M_k given by

$$M_k = \langle\Psi(0)|H^k|\Psi(0)\rangle. \quad (15)$$

The fundamental property of the effective-mode formalism is contained in the following: *Using the system's modes augmented by n members of the hierarchy of effective Hamiltonians, one reproduces exactly all the moments M_k of the entire macrosystem with $k \leqslant 2n + 1$.* This property has been proven for the use of the first member of the hierarchy in Ref. [33]. For the more recent inclusion of higher members of the hierarchy, the property has been proven analytically in Ref. [44]. In the latter reference, the general case where more than two electronic states are involved (multi-state conical intersections) is also considered. The exactness of

the lowest moments is a property of central interest: it tells us that by using a few members of the hierarchy only, *i.e.*, by using a truncated environment, one nevertheless reproduces numerically exactly the dynamics of the entire macrosystem on a limited time-interval. By numerically exact we mean that, since we are dealing with a time-expansion, the results are considered exact on a time-range where the neglected part of the environment has an impact below a given error criterion. The time up to when this impact stays below an acceptable error defines the corresponding time-scale which is not known *a priori* and depends on all the parameters of the problem.

With only the first member of the hierarchy (and the system), one gets exactly the first four moments of the macrosystem (M_0 to M_3, but only M_2 and M_3 are not trivial). In the Taylor expansion, this corresponds to the very short-time dynamics. With the addition of the second member of the hierarchy two more moments, M_4 and M_5 become exact, and the dynamics will be accurate on a longer time-scale, etc. Thus, the sequential coupling of the members of the hierarchy translates into a sequential description of the dynamics. At each time an additional member comes into play, the energy is further spread within the environment. We stress that this property is intimately related to the hierarchy of effective Hamiltonians. Using the original Hamiltonian instead, all the N_B modes of the environment participate in the dynamics whatever the time-scale is, excluding a numerically exact treatment of the dynamics even for short times.

The dynamical properties are furthermore closely connected to spectral properties. Indeed, the spectrum of the macrosystem $P(E)$ corresponds to the Fourier transform of the autocorrelation function:

$$P(E) \propto \int \mathrm{d}t C(t) \mathrm{e}^{\mathrm{i}Et}. \tag{16}$$

Accordingly, the moments of the autocorrelation function are connected to properties of the spectra. For instance, M_1 gives the center of gravity of the spectrum, M_2 is related to the width of the spectrum, M_3 to the main asymmetry, etc. As a consequence, using a truncated hierarchy of effective Hamiltonians, one can obtain the spectra of the entire macrosystem at a given resolution. These spectra can be compared to experimental ones. When more members of the hierarchy are included in a calculation, more resolved spectra can be accurately reproduced. These properties have been illustrated with numerical examples in Ref. [43] and will be further illustrated in the examples to be presented below in Section 3.

Unless the complete hierarchy is constructed a residual environment subsists. This residual environment has no impact on the time-scale correctly reproduced by the members of the hierarchy included in a calculation of the dynamics but plays a role at later times, when the dynamics provided by the use of a limited number of members of the hierarchy will no longer be accurate. Of course, to obtain the numerically exact quantum dynamics on an arbitrary large time-scale one must fully include the residual environment, but this is generally out of reach due to the large number of residual modes. However, one can nevertheless include the residual environment in an approximate manner, as will be done in our numerical examples. Clearly, the results on the time-scale where the residual environment has no impact will not be affected by the approximation whatever it is, and one can only expect changes on the longer time-scale. In the following, we present the wavepacket propagation technique used in this study, as well as the approximation used to include additionally the residual environment in the quantum dynamics of the macrosystem.

2.2. Wavepacket propagation technique and approximate dynamics

To calculate numerically the quantum dynamics of the macrosystem, we shall use the multiconfiguration time-dependent Hartree method (MCTDH) [19–22]. This method for propagating multidimensional wave packets is one of the most powerful techniques currently available. The MCTDH method, to be briefly exposed below, relies on a multiconfigurational form of the wavepacket. If enough configurations are included, the results are numerically exact. For conical-intersection situations, MCTDH is able to treat problems involving about 20–30 modes [15,23–28]. In practice, we will thus treat with MCTDH the system modes plus a few members of the hierarchy of effective Hamiltonians, up to a total of 20–30 modes. If the members of the hierarchy of effective Hamiltonians added to the system suffice to reproduce accurately the dynamics on the time-scale under intersect, then the residual environment can be neglected. However, if this is not the case, the latter should be included, and then, an exact treatment of the dynamics, even with MCTDH, may no longer be feasible.

To include even more modes in the wavepacket propagation, *i.e.*, in the present case, in view of including the residual environment, one could (and must) use an approximate technique. Here, we shall exploit the MCTDH method by using a reduced number of configurations. In the limit of a single configuration for the residual modes, we recover the time-dependent Hartree approximation (TDH) [48,49], which has the advantage of small numerical requirements and allows to include a very large number of modes.

2.2.1. The multiconfiguration time-dependent Hartree (MCTDH) method

The MCTDH method [19–22] uses a variationally optimized time development of the wavefunction expanded in a basis of sets of time-dependent functions called single-particle functions (SPFs). Details of the method can be found in Refs. [21,22], but to be self-contained we briefly present the equations of motion for the expansion coefficients and the SPFs. A set of SPFs is used for each particle, where

each particle represents a coordinate or a set of coordinates called combined mode. Indeed, when some modes are strongly coupled, and when there are many degrees of freedom, it is more efficient to combine sets of coordinates together as a "particle" with multidimensional coordinate $q_\kappa = (x_i, x_j, \ldots)$ [14]. Consequently, the number of particles, p, must be distinguished from the total number of modes of the macrosystem $N = N_S + N_B$.

The MCTDH wavefunction ansatz for N modes combined as p particles is the multiconfigurational expansion

$$\Psi(x_1, \ldots, x_N, t) \equiv \Psi(q_1, \ldots, q_p, t), \tag{17}$$

$$= \sum_{j_1}^{n_1} \cdots \sum_{j_p}^{n_p} A_{j_1 \ldots j_p}(t) \prod_{\kappa=1}^{p} \varphi_{j_\kappa}^{(\kappa)}(q_\kappa, t), \tag{18}$$

$$= \sum_{J} A_J \phi_J, \tag{19}$$

where n_κ is the number of SPFs for the κth particle and where the third line defines the multi-index $J = (j_1 \ldots j_p)$ and the configuration $\phi_J = \varphi_{j_1}^{(1)} \varphi_{j_2}^{(2)} \ldots \varphi_{j_p}^{(p)}$.

To obtain the set of coupled equations of motion for the coefficients and SPFs, the Dirac–Frenkel variational principle is used. Dividing the Hamiltonian into parts that act only on a given particle (separable terms), and a rest, correlated term

$$H(q_1, \ldots, q_p) = \sum_{\kappa=1}^{p} h_\kappa(q_\kappa) + H_R(q_1, \ldots, q_p), \tag{20}$$

one obtains the equations of motion [20–22]:

$$i\dot{A}_J = \sum_L \langle \phi_J | H_R | \phi_L \rangle A_L, \tag{21}$$

$$i\dot{\varphi}_a^{(\kappa)} = h_\kappa \varphi_a^{(\kappa)} + (1 - P^{(\kappa)}) \sum_{b,c}^{n_\kappa} \rho_{ab}^{(\kappa)^{-1}} \mathscr{H}_{bc}^{(\kappa)} \varphi_c^{(\kappa)}, \tag{22}$$

where $\mathscr{H}_{bc}^{(\kappa)} = \langle \Psi_b^{(\kappa)} | H_R | \Psi_c^{(\kappa)} \rangle$ is the mean-field matrix operator, with the "single-hole function" $\Psi_a^{(\kappa)}$

$$\Psi_a^{(\kappa)} = \langle \varphi_a^{(\kappa)} | \Psi \rangle = \sum_{j_1}^{n_1} \cdots \sum_{j_{\kappa-1}}^{n_{\kappa-1}} \sum_{j_{\kappa+1}}^{n_{\kappa+1}} \cdots \sum_{j_p}^{n_p} A_{j_1 \cdots j_{\kappa-1} a j_{\kappa+1} \cdots j_p}, \tag{23}$$

$$\times \varphi_{j_1}^{(1)} \cdots \varphi_{j_{\kappa-1}}^{(\kappa-1)} \varphi_{j_{\kappa+1}}^{(\kappa+1)} \cdots \varphi_{j_p}^{(p)}, \tag{24}$$

which collects all the terms in the wavefunction which would contain the ath function of the κth particle. $P^{(\kappa)} = \sum_a |\varphi_a^{(\kappa)}\rangle\langle\varphi_a^{(\kappa)}|$ is the projector on the set of SPFs for the κth particle, and $\rho^{(\kappa)}$ is the reduced density matrix defined by $\rho_{ab}^{(\kappa)} = \langle \Psi_a^{(\kappa)} | \Psi_b^{(\kappa)} \rangle$. These equations of motion are general, and can also be used to treat the dynamics of nonadiabatic systems. In this case on introduces an electronic degree of freedom to label the electronic states. The corresponding SPFs for this "degree of freedom" thus takes only discrete values [21,50,53]. In general, however, one can improve the efficiency of the MCTDH method for vibronically coupled systems by writing the MCTDH wavefunction as a sum of several wavefunctions – one for each electronic state – which use different sets of SPFs [14,21]:

$$\Psi(t) = \sum_{\alpha}^{n_s} \Psi(q_1, \ldots, q_p, \alpha, t) |\alpha\rangle \tag{25}$$

with

$$\Psi(q_1, \ldots, q_p, \alpha, t) = \sum_{J_\alpha} A_{J_\alpha}^{(\alpha)} \phi_{J_\alpha}^{(\alpha)}, \tag{26}$$

where n_s is the number of electronic states, and J_α is the multi-index for the configurations used to describe the wavefunction on the state α. This form of the MCTDH wavefunction has the advantage to allow for a separate optimization of the SPFs for each electronic state, and therefore fewer coefficients are needed in the wavefunction expansion. This choice is employed in this work, and the equations of motion using this *multi-set* form of the wavefunction become

$$i\dot{A}_{J_\beta}^{\beta} = \sum_{\alpha}^{n_s} \sum_{L_\alpha} \langle \phi_{J_\beta}^{(\beta)} | H_R^{\beta,\alpha} | \phi_{L_\alpha}^{(\alpha)} \rangle A_{L_\alpha}^{(\alpha)}, \tag{27}$$

$$i\dot{\varphi}_a^{(\beta,\kappa)} = h_\kappa^{(\beta)} \varphi_a^{(\beta,\kappa)} + (1 - P^{(\beta,\kappa)}) \times \sum_{b}^{n_\kappa^{(\beta)}} \sum_{c}^{n_\kappa^{(\alpha)}} \sum_{\alpha}^{n_s} \rho_{ab}^{(\beta,\kappa)^{-1}} \mathscr{H}_{bc}^{(\beta,\alpha,\kappa)} \varphi_c^{(\alpha,\kappa)}, \tag{28}$$

where α and β refer to the various electronic states.

The solution of the equations of motion requires the computation of the mean-fields at every time-step. The efficiency of the MCTDH method thus demands their fast evaluation, and necessitates to avoid the explicit calculation of high-dimensional integrals. Using the form of the Hamiltonian given by Eq. (20), we readily see that the evaluation of the mean-fields for the separable terms needs only integrals over a single particle at a time. However, for the correlated part of the Hamiltonian, H_R of Eq. (20), the mean-fields may involve integrals of the full dimensionality of the problem. This correlated term can, however, be written as a sum of products of single-particle Hamiltonians, rendering the evaluation of the mean-fields faster:

$$H_R = \sum_{r=1}^{s} c_r \prod_{\kappa=1}^{p} h_r^{(\kappa)}, \tag{29}$$

where $h_r^{(\kappa)}$ operates on the κth particle only and where the c_r are numbers.

Interestingly, the LVC Hamiltonian H_B used to describe the environment in this work is already in this form, allowing a powerful use of the MCTDH method. The transformed versions of this Hamiltonian written as the sum of a few members of the hierarchy of effective Hamiltonians plus a residual environment, $\sum_{m=1}^{n} H_m + H_{rn}$, are also appropriate for the use of MCTDH; the correlated term of the Hamiltonian of the environment is given as a sum of products of two-particle Hamiltonians, corresponding to the bilinear coupling terms in the Hamiltonians H_m and H_{rn} of Eqs. (11) and (12).

2.2.2. The single-configuration approximation for the residual environment

The numerical requirement of the MCTDH method have been discussed in details in Refs. [14,21]. The increasing number of expansion coefficients and SPFs with the number of degrees of freedom leads to the typical limit of 20–30 modes which can be treated with a reasonable numerical effort in conical-intersection situations. (As already noted, with the multi-layer extension of MCTDH recently developed by Wang and Thoss, one may push this limit a bit further [29,30].) In this work, we study the possibility to treat the system's modes and a few effective modes with the proper number of configurations (*i.e.*, in a multiconfiguration form), and treat additionally the modes of the residual environment by employing a single configuration, which amounts to describe the residual environment by the TDH approximation.

The equations of motion using the proposed scheme to include the residual environment are exactly those of MCTDH given above, and only the numbers of SPFs and expansion coefficients are drastically reduced compared to what would require a full multiconfigurational expansion for the entire macrosystem. Within the multi-set MCTDH formalism, the minimal number of configurations for the residual environment is one per electronic state, *i.e.*, the total wavefunction takes on the appearance:

$$\Psi(t) = \begin{pmatrix} \Psi^{(1)}_{\mathrm{S+eff}} \Psi^{(1)}_{\mathrm{RE}} \\ \Psi^{(2)}_{\mathrm{S+eff}} \Psi^{(2)}_{\mathrm{RE}} \end{pmatrix}, \tag{30}$$

with $\Psi^{(\alpha)}_{\mathrm{S+eff}}$ being the multiconfigurational wavefunction of the system part and of the effective modes and $\Psi^{(\alpha)}_{\mathrm{RE}}$ the single-configuration wavefunction for the residual environment (RE) for the state α. Note that this approach is equivalent to the independent-state Hartree (ISH) approximation discussed in Ref. [50]. Using this form of the wavefunction, the dynamics provided by the system's modes augmented by the effective modes is numerically exact as long as the use of the effective modes suffices to reproduce the dynamics of the entire macrosystem. The impact of the residual environment, treated approximately, becomes relevant only at later times. The use of the TDH approximation amounts to completely neglect the correlation between the modes, and usually fails to represent the dynamics correctly. However, if the coupling of the residual environment is small, the Hartree approximation is expected to provide a reasonable description of the dynamics of these modes.

3. Numerical examples

The effective-mode formalism can be used to describe the dynamics of very large system–environment complexes because the environment is reduced to a few effective modes, possibly augmented by the residual environment treated approximately. However, in order to assess the quality of the approach, we need to compare the results given by the effective-mode formalism to those obtained from the full Hamiltonian. That is, we need to solve the exact problem. Of course, this drastically restricts the number of modes which can be included in the two examples presented below. While, within our approach, the dynamics provided by the system modes plus some effective modes up to a total of 20–30 modes can be treated "exactly" and augmented by the (potentially many) residual modes using the TDH approximation, we are restricted here to a somewhat smaller total number of modes. Consequently, our two examples will involve, respectively, 22 and 24 modes in total, allowing for a numerically exact treatment of the full Hamiltonians. The objective is twofold: examine (i) the performance of the hierarchy of effective modes, and (ii) the impact of the additional inclusion of the residual environment treated by the TDH approximation.

3.1. Calculated quantities

We will present autocorrelation functions, spectra at various resolutions, and diabatic populations. The autocorrelation function $C(t)$ of the macrosystem is given by Eq. (13). Since our Hamiltonians are symmetric and the initial wavepackets are real, one can exploit the following useful formula [54,55]

$$C(t) = \langle \Psi(t/2)^* | \Psi(t/2) \rangle, \tag{31}$$

which allows to reduce the propagation time by a factor of two. The autocorrelation function is directly obtained from the propagated wavepacket.

By Fourier transformation, the autocorrelation function gives the spectrum of the macrosystem, see Eq. (16). Due to our finite propagation time T, the Fourier transformation causes artifacts known as the Gibbs phenomenon [56]. In order to reduce this effect, the autocorrelation function is multiplied by a damping function $cos^2(\pi t/2T)$ [15,21]. To simulate the experimental line broadening, the autocorrelation functions will be damped by an additional multiplication with a Gaussian function

$$\exp[-(t/\tau)^2], \tag{32}$$

where τ is the damping parameter. This multiplication is equivalent to a convolution of the spectrum with a Gaussian with a full width at half maximum (FWHM) of $4(\ln 2)^{1/2}/\tau$. The convolution simulates the resolution of the spectrometer used in experiments.

The other quantities we want to evaluate are the time-evolving (diabatic) electronic populations, $P_\alpha(t)$. These populations are defined as follows:

$$P_\alpha(t) = \langle \Psi(q_1, \ldots, q_p, \alpha, t) | \Psi(q_1, \ldots, q_p, \alpha, t) \rangle, \tag{33}$$

where the wavefunction for the state α is given by Eq. (26).

3.2. Model system–environment complex

Since we separate a system part from the environment part, and want the latter to be as large as possible, we

aim to identify a suitable model system which features a system part that is as small as possible: in particular, a two-mode system giving rise to a CI. As an appropriate case, we choose the 2-mode model derived to study the dynamics of the ground and first excited states of the butatriene cation ($C_4H_4^+$) [57,1]. This prototypical model comprises one tuning mode and one coupling mode. We mention that the quantum dynamics of the butatriene cation in its full dimensionality (18 modes), using the second-order vibronic coupling model have been studied [23]. Our approach is designed for LVC environments, and, in the present study, the basic two-mode model is coupled to an – hypothetical – environment consisting of 20 modes. The environment is a model determined by realistic choices of the parameters appearing in H_B, Eq. (3), but is not expected to simulate the neglected intramolecular modes of butatriene.

This example is similar to the first one discussed in Ref. [35]. In the latter reference, only the first member of the hierarchy of effective Hamiltonian was employed. We shall here include additional members of the hierarchy and treat the residual environment by TDH. All the calculations to be reported in this work were carried out using the Heidelberg Package of MCTDH [58].

For this example, each member of the hierarchy of effective Hamiltonians is comprised of three effective modes. This corresponds to the most general situation of the effective-mode formalism for two electronic states, and we shall discuss the results in details. The parameters of the 2-mode system are taken from Refs. [57,1] and those of the environment from Ref. [35]. They are collected in Table 1.

In the following, we shall present results for six different cases: (i) 2-mode system alone, (ii) system augmented by the original environment treated by TDH, (iii) system plus one member of the hierarchy of effective Hamiltonians (3 effective modes), (iv) system plus two members of the hierarchy (6 effective modes), and cases (v) and (vi) which are similar to cases (iii) and (iv), respectively, but augmented by the corresponding residual environment treated by the TDH. All the results are compared to exact ones, obtained by propagating the full multiconfigurational wavefunction of the 22-mode system–environment complex. The parameters corresponding to our various cases are collected in Tables 1–3. The propagation time T is 100 fs, thus allowing to calculate autocorrelation functions up to 200 fs using Eq. (31).

In the following, to simplify the notation, we shall abbreviate effective mode by EM and the residual environment treated with the TDH approximation by HRE – for Hartree residual environment.

3.2.1. Autocorrelation function

Fig. 1 presents the absolute value of the autocorrelation functions for the six cases mentioned above, along with the exact one for comparison. An initial excitation to the upper electronic state is considered. The figure is composed of four panels. Panel A shows the autocorrelation functions for the system alone and the system plus the original environment treated with TDH. Panel B compares the use of the system plus 3 or 6 effective modes, neglecting the residual environment. Panel C (D) presents the results for the system plus 3 (6) effective modes, augmented or not by the 17 (14) residual modes treated with TDH. In all panels the exact result is shown for comparison. Pay attention to the ordinate-scale which is chosen to emphasize the tail of the autocorrelation functions: for panel A, this scale is however 10 times larger than in the three other panels! Of course, at $t = 0$, the value of the autocorrelation functions is unity.

Let us first discuss panel A, showing the results for the system alone, the system plus TDH and the exact one. We see the very important impact of the environment.

Table 1
Parameters of the original Hamiltonian for the first example

Label	ω_i	$\kappa_i^{(1)}$	$\kappa_i^{(2)}$	λ_i
ν_g	0.258	−0.212	0.255	
ν_u	0.091			0.318
1	0.2753	−0.0318	−0.0367	
2	0.1508	−0.0782	−0.0325	
3	0.1413	0.0445	−0.0693	
4	0.1206	0.0583	0.0768	
5	0.0980	0.0803	−0.0667	
6	0.0828	0.0646	−0.0754	
7	0.0732	0.0512	0.0676	
8	0.0809			−0.0440
9	0.0716			−0.0704
10	0.0568			−0.0323
11	0.0539			−0.0478
12	0.0443	−0.0200	−0.0219	−0.0204
13	0.0400	−0.0110	0.0100	−0.0152
14	0.0358	−0.0156	−0.0155	−0.0147
15	0.0301	−0.0136	−0.0160	0.0099
16	0.0279	−0.0153	0.0166	−0.0052
17	0.0262	0.0142	−0.0123	−0.0055
18	0.0229	0.0155	−0.0100	−0.0074
19	0.0216	−0.0119	0.0141	−0.0098
20	0.0197	0.0113	0.0115	0.0081

The mode-label ν_g and ν_u represent the tuning and coupling modes of the system, respectively. The vertical energy split is $E_2 - E_1 = 0.4$ eV. The system's parameters are taken from Ref. [1]. The parameters for the model environment are taken from Ref. [35].
All values are given in eV.

Table 2
Parameters of the first and second members of the hierarchy of effective Hamiltonians, H_1 and H_2, for the first example

H_1	Ω_i	$K_i^{(1)}$	$K_i^{(2)}$	Λ_i
1	0.0644	0.0642	0.0241	0.9998
2	0.1002	0.6089	−0.8235	−0.0084
3	0.1274	−0.7907	−0.5667	0.0181
$\bar{\kappa}^{(1)} = 0.1666$		$\bar{\kappa}^{(2)} = 0.1728$		$\bar{\lambda} = 0.1074$
H_2	Ω_j	d_{1j}	d_{2j}	d_{3j}
4	0.0517	0.0139	0.0012	−0.0042
5	0.1002	−0.0008	−0.0287	0.0151
6	0.1846	−0.0014	0.0130	0.0587

All values are in eV.

Table 3
Parameters of the residual environments H_{r1} and H_{r2} for the first example

j	H_{r1}				H_{r2}			
	ω_j	d_{1j}	d_{2j}	d_{3j}	ω_j	d_{4j}	d_{5j}	d_{6j}
4	0.0206	−0.0026	0.0015	0.0062	–	–	–	–
5	0.0224	0.0040	0.0039	0.0000	–	–	–	–
6	0.0238	−0.0015	0.0050	−0.0024	–	–	–	–
7	0.0269	−0.0024	0.0040	−0.0014	0.0220	0.0020	−0.0001	−0.0094
8	0.0302	0.0007	0.0134	−0.0031	0.0244	0.0015	−0.0041	−0.0007
9	0.0317	−0.0038	0.0001	−0.0086	0.0250	0.0059	−0.0013	−0.0016
10	0.0373	0.0022	−0.0017	−0.0078	0.0283	0.0053	0.0010	−0.0026
11	0.0412	0.0037	0.0063	−0.0001	0.0362	0.0064	−0.0035	0.0091
12	0.0474	0.0042	−0.0008	−0.0119	0.0391	0.0010	−0.0020	−0.0119
13	0.0558	−0.0028	−0.0001	0.0005	0.0436	−0.0104	−0.0115	−0.0110
14	0.0615	0.0090	0.0001	−0.0007	0.0530	−0.0041	−0.0024	0.0209
15	0.0788	−0.0048	−0.0000	−0.0003	0.0564	−0.0026	−0.0059	0.0045
16	0.0884	−0.0008	−0.0049	0.0152	0.0592	−0.0025	0.0386	−0.0055
17	0.0933	−0.0009	0.0093	0.0234	0.0758	−0.0078	0.0014	0.0004
18	0.1297	0.0004	0.0214	−0.0047	0.0957	0.0001	−0.0205	−0.0046
19	0.1515	0.0009	0.0049	−0.0298	0.1186	−0.0010	−0.0012	−0.0413
20	0.2623	0.0009	−0.0111	−0.0409	0.1891	−0.0018	0.0145	−0.0664

All values are in eV.

The strong recurrences of the system's autocorrelation function are washed out, and the absolute value of the autocorrelation function becomes very small after the initial decay. When we treat the environment by TDH, we see that the system's recurrences are partly washed out, but clearly are still too strong. Furthermore, while the very short initial decay seems rather well reproduced over the first 5 fs (only), after that time the oscillating features of the autocorrelation function appear physically meaningless. Clearly, the TDH approximation for the original environment cannot properly simulate the impact of the latter onto the system.

In panel B we compare the use of 3 and 6 effective modes to simulate the environment. We see that the use of 3 EM suffices to reproduce very accurately the dynamics of the entire complex up to 15 fs, at which point the ultrafast decay of the autocorrelation function is nearly complete. Such ultrafast decay is typical for CI situations, and the use of 3 EM suffices to describe it correctly. Note that this decay has non-trivial structures already before 15 fs, as can be seen from the exact result in panel A where the ordinate-scale is 10 times larger. These structures are not correctly reproduced by the TDH approximation for the original environment (panel A) but with 3 EM they are described properly. At longer times, *i.e.*, after the initial decay, the dynamics is no longer accurately reproduced by the effective modes, as expected due to the neglect of the residual modes. In particular, one sees that the 3-EM autocorrelation function assumes too high values after the initial decay. This simply indicates that the reduced dimensionality of the environment, 3 EM instead of the original 20 modes, typically allows for a larger overlap of the initial wavefunction with the time-evolving one than in the full-dimensional problem. We compare here a 5-dimensional calculation (2-mode system + 3EM) to a 22-dimensional one!

To account for the spreading of the wavepacket in more directions of the environment we add three additional effective modes. We thus have 6 EM, and, according to the dynamical property of the effective modes, the dynamics must be accurate on a longer time-scale. This is indeed the case as can be seen in Fig. 1B: the dynamics is very accurately reproduced up to roughly 30 fs now. Again, for longer times the influence of the neglected modes becomes important. Note however that the structures around 50 fs are quite well reproduced, even though there is an error in the amplitudes. Again, this contrasts drastically with the treatment of the original environment by TDH (panel A), where the oscillations are meaningless and their amplitude four times larger than in the effective-mode results.

Comparing the 3-EM results to the 6-EM ones (panel B), we see that the structures after the initial decay of the autocorrelation functions change. Clearly, the structures between 20 and 40 fs are significantly better reproduced when using six effective modes, as expected from the theory. We can also compare the autocorrelation function at longer times, where none of the effective-mode results can be expected to be very accurate since this time-range exceed their respective time-scale of good accuracy. In particular, between 60 and 90 fs we see that, while the 3-EM autocorrelation function exhibit a strong, artificial, recurrence, the latter disappears in the 6-EM case. In the 6-EM case, artificial recurrences appear at roughly 50, 100 and 150 fs, and in between the amplitude of the exact autocorrelation function is quite well reproduced. By contrast, the 3-EM autocorrelation function exhibit too strong recurrences at almost all times after 15 fs.

Next we investigate the influence of the residual environment when used on top of the effective modes and treated approximately by TDH. Obviously, if the residual environment is treated exactly we recover the exact results. We

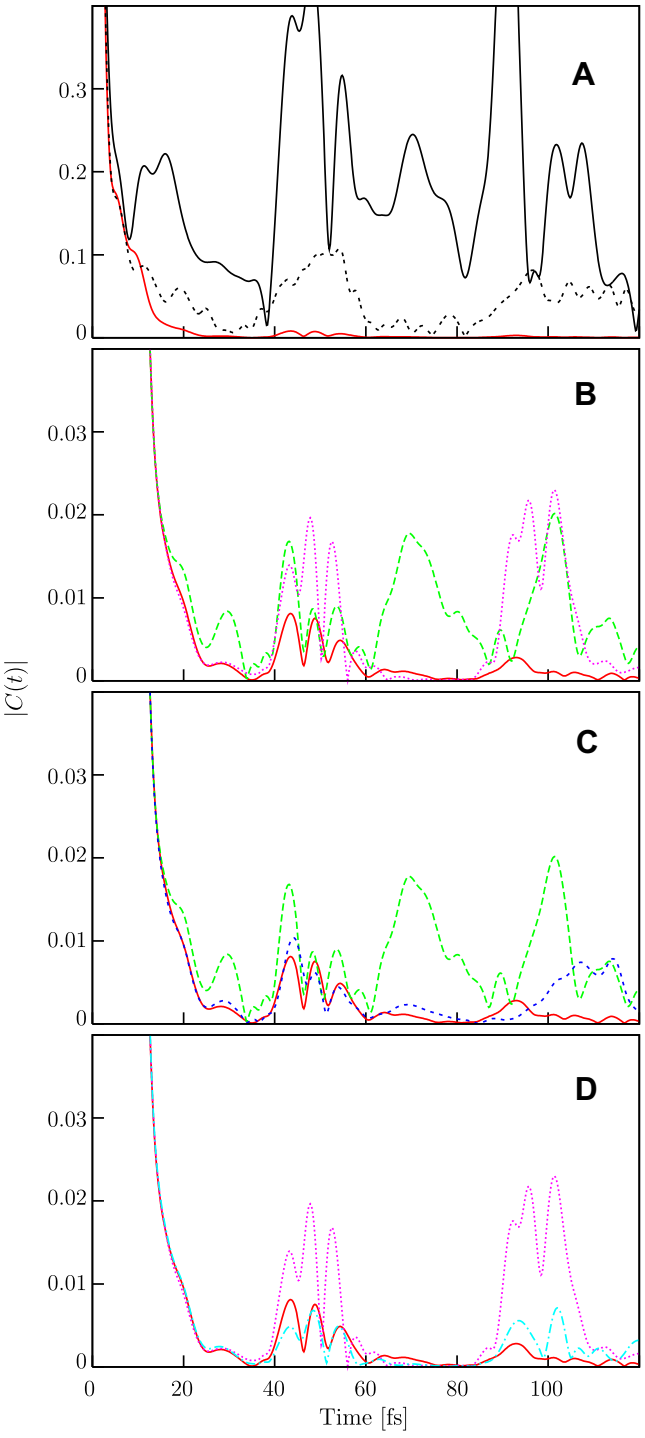

Fig. 1. Absolute value of the autocorrelation functions as a function of time for the first example. The figure contains four panels. Note that the ordinate-scale is ten times larger for panel A than for the other panels. The line-coding is the same for all panels. (Red, in all panels) full line: exact 22-dimensional result. (Black, uppermost line in panel A) full line: system alone. (Black, only in panel A) dashed line: system plus TDH approximation for all the original modes of the environment. (Green) long-dashed line: system plus 3 effective modes (EM). (Pink) dotted line: system plus 6 EM. (Dark blue) short-dashed line: system plus 3 EM plus the 17-mode Hartree residual environment (HRE). (Light-blue) dashed-dotted line: system plus 6 EM plus 14-mode HRE. Panel A shows the result for the system alone and the system plus the original environment treated by TDH. Panel B compares the exact result to the one obtained with the system plus 3 or 6 EM. Panel C shows the effect of treating the HRE for the system plus 3 EM case. Panel D is similar to panel C but obtained with the system plus 6 EM. (For interpretation of the references in color in this figure legend, the reader is referred to the web version of this article.)

start by considering panel C of Fig. 1, which compares the 3-EM results obtained with and without the Hartree residual environment (HRE). We see that the improvement is indeed very good: the autocorrelation function with HRE follows correctly the exact one up to 80 fs. The results in the time-range between 15 and 40 fs is particularly well improved. Importantly also, the artificial recurrence of the 3-EM result around 70 fs is washed out. The HRE, which allows for the wavefunction to spread into all directions of the environment, but neglect all correlations between the residual modes and the effective modes, provides a clear improvement of the overall behavior of the autocorrelation function. When comparing the results for 6EM and 6EM + HRE, panel D, similar conclusions hold. In particular, the intensity of the recurrence around 100 fs of the 6-EM result is significantly decreased and is now reasonably close to the exact one.

The action of the HRE is mainly to decrease the intensity of the (artificial) recurrences and improves the EM results on the intermediate and long times. We want to recall that only the tail of the autocorrelation functions are shown: the absolute error is indeed small in all effective-mode cases. We turn now to the discussion of the spectra obtained by Fourier transform of the autocorrelation functions.

3.2.2. Spectra

Fig. 2 presents the spectra obtained from the autocorrelation functions. The spectra discussed here correspond to the sum of two contributions: one obtained from a wavepacket propagation starting on the upper electronic state, and one from the lower state. We discuss the summed spectra rather than the two contributions individually. The figure contains again four panels. In panel A, the exact spectrum is compared to the one obtained by treating directly the original environment by TDH. (The much more structured spectrum of the system alone is not shown.) In panel B (C) we compare the spectra of the 3 (6) EM calculations, with and without the corresponding HRE. Panel D compares directly the 3EM + HRE result to the 6EM + HRE one. In all panels the exact spectra are shown for comparison. The coding of the various lines follows the one used for the autocorrelation functions (see Fig. 1.) For all spectra, the autocorrelation functions have been further multiplied by a Gaussian with damping parameter $\tau = 77$ fs for panel A, B and C, and $\tau = 155$ fs for panel D, see Eq. (32). This corresponds to the convolution of the spectra with a Gaussian of FWHM of 30 and 15 meV, respectively.

In panel A, we see that the wrong result for the autocorrelation function when the original environment is treated

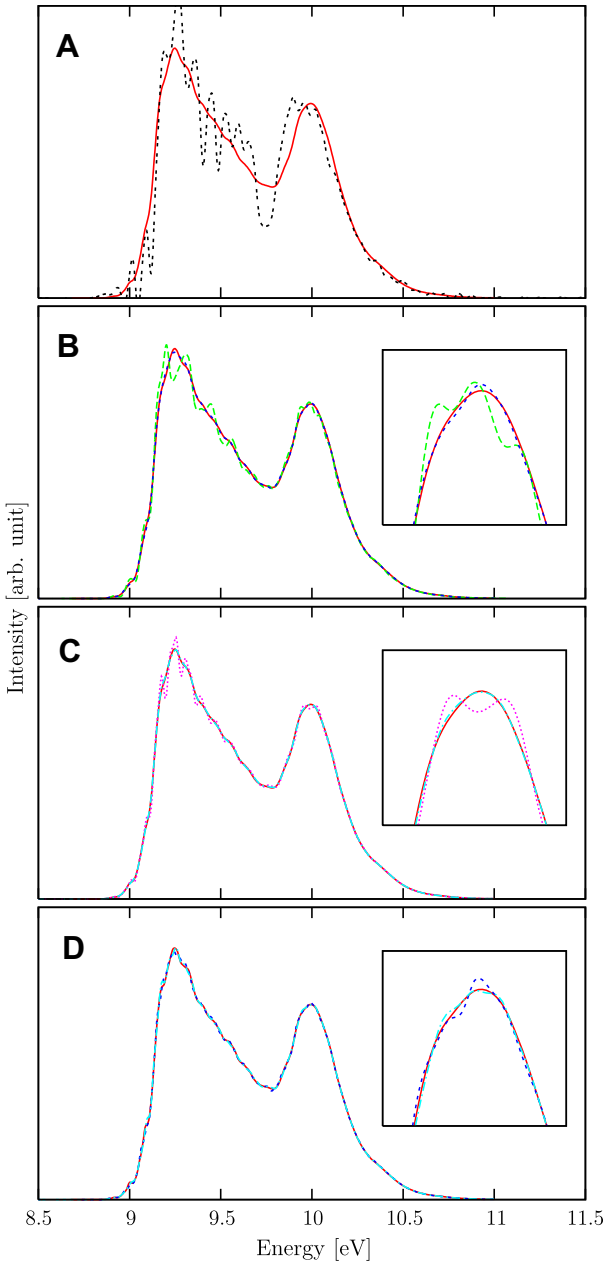

Fig. 2. Spectra as a function of the energy at various resolutions for the first example. The figure contains four panels. The coding of the line is the same as for Fig. 1 (see the corresponding caption). Panel A compares the exact result to the one for the system plus the original environment treated by TDH (the system alone is not shown). The insets in panels B, C, and D zooms the high-energy peak of the spectra. Panel B compares the exact spectrum with the one obtained using the system plus 3 effective modes (EM) augmented or not by the Hartree residual environment (HRE). Panel C compares the exact spectrum with the one obtained using the system plus 6 EM augmented or not by the HRE. Panel D compares the exact spectrum with the one obtained using the system plus 3EM + HRE and system plus 6EM + HRE. The resolution for panels A, B, and C is 30 meV, in panel D it is 15 meV. Some of the lines are difficult to distinguish from the exact results. See text for details.

by TDH translates into a wrong spectrum. Clearly, the structures are not only too much pronounced but simply incorrect. This is particularly true for the high-energy peak, where the nonadiabatic effects are most important. This peak is not at the correct position. Even when using a damping parameter of 10 fs corresponding to the convolution of the spectrum by a Gaussian of FWHM $\simeq$ 220 meV, this peak is at too low energy (not shown). Furthermore, the width of the spectrum, which is related to the second moment, is not correct. Since the second moment is the first non-trivial one, this tells us that even the ultrafast decay of the autocorrelation function is not sufficiently correctly reproduced. This will contrast with the effective-mode results, where the use of the first member of the hierarchy of effective Hamiltonians warrants that the second moment and thus the width of the spectrum is exactly reproduced.

Panel B displays the 3-EM result along with the 3EM + HRE one. Note that the 3-EM result coincides with the exact one at a low resolution of 110 meV ($\tau = 20$ fs), see Ref. [35]. At higher resolutions deviations occur, mainly due to the too strong recurrences of the autocorrelation function compared to the exact one. These recurrences carve too strongly the shape of the spectrum. However, this shape is quite well reproduced even at this higher resolution. Clearly, the fact that the HRE diminishes the artificial recurrences of the effective-mode autocorrelation function allows to better reproduce the spectrum, and, at the resolution of 30 meV (panel B), differences with the exact one can hardly be observed (see also the inset, which zooms the high-energy peak of the spectra). The HRE thus allows to increase the resolution for which the spectrum is reproduced accurately by almost a factor of 4.

For panel C, the conclusions are similar: the use of the HRE improves the spectrum provided by the 6 EM. We remark that no difference is visible between the exact and the 6-EM spectra at a resolution of 50 meV (not shown). We can, of course, also compare directly the 3-EM result of panel B with the 6-EM result of panel C. At this higher resolution of 30 meV, we clearly see the improvement provided by the additional use of the second member of the hierarchy. This is particularly true in the middle of the band and for the low energy peak.

In panel D, the 3EM + HRE and 6EM + HRE spectra are compared at an even higher resolution of 15 meV. We see that the 6EM + HRE result is slightly better than the 3EM + HRE one, see the inset, as is expected from inspection of the autocorrelation functions. The 6EM + HRE spectrum is almost indistinguishable from the exact one. Note that this resolution corresponds to a damping time, Eq. (32), of 155 fs, a time-range for which none of the autocorrelation functions are highly accurate. Nevertheless, the exact spectrum is very well reproduced using the effective modes, and even better reproduced by the additional inclusion of HRE. Note also that when doubling the resolution from panel B to C, the exact spectrum is only slightly more structured. This is a typical feature of the presence of CI in a multidimensional system: the spectrum is congested and individual spectral lines are hard to resolve even at high resolutions. The effective modes, augmented by HRE,

reproduce very well the spectral envelope in such situations, while the direct use of TDH for the environment fails.

3.2.3. Discussion

With this numerical example we see that the dynamics is accurately reproduced on a short-time-scale by using only three effective modes to represent the environment. The time-range of accuracy is increased when three additional effective modes are used, corresponding to a truncation of the hierarchy of effective Hamiltonians at second order. These results are in complete accordance with the theoretical predictions [18,33,44].

Regarding the autocorrelation functions, the use of a reduced number of effective modes leads to artificial recurrences after the time-range of accuracy. This can be understood by considering the dimensionality of the problem: the neglect of the residual environment suppresses the possibility for the nuclear motion to explore the full-dimensional space, resulting in an increased overlap between the initial wavepacket and the time-evolving one. By allowing the macrosystem to explore the full space, even using an approximate treatment for the residual environment, this overlap is decreased and the values of the autocorrelation functions become closer to the exact one over the whole time-range studied. For this example, the neglected correlations between the residual modes seem not to play a crucial role, and spectra with higher resolutions can be accurately obtained by using only one or two members of the hierarchy of effective Hamiltonian augmented by the HRE – for instance, from 110 meV to 30 meV when using three effective modes and adding the HRE. Finally, we mention that the use of HRE also improves the electronic-state population dynamics provided by the effective modes over the entire time-range.

By contrast, TDH fails to represent properly the original environment. This means that the correlation do play a crucial role for the original environment and cannot be neglected without strongly altering the quality of the results. Using the effective-mode formalism, a relevant part of the correlation is properly accounted for, as well as cumulative effects of the full environment. The addition of the HRE is then of much better quality, and help to improve the effective-mode results globally over the full time-range.

We make a last remark regarding the numerical requirements. For this example, the exact calculation required 3.8 Gbytes of memory, and, for comparison, the 6-EM one 250 Mbytes and the 6EM + HRE one 260 Mbytes. These values are obtained for calculations which satisfied very strict convergence criteria, because we wanted to be on safe grounds when comparing results with very small differences. To add more modes to the full calculation will quickly requires a too large amount of memory, even when using MCTDH. In contrast, the effective modes are build from all the modes of the environment, and can thus simulate an arbitrarily large one. The effective coupling constants will grow with the number of environmental modes, increasing accordingly the requirements for numerical convergence, but the number of effective modes remains the same avoiding the scaling problem. To add the HRE on top of the effective modes adds a very moderate cost. Thus, the effective modes, augmented by the HRE, can be used to simulate the dynamics of macrosystems with a truly large number of modes.

3.3. $S_2 - S_1$ conical intersection in pyrazine: model intramolecular environment

For our second example, we study the $S_2 - S_1$ conical intersection of the pyrazine molecule, using a model intramolecular environment. This model has been proposed by Krempl et al. [51] and is of very particular nature. The pyrazine molecule is described by a 4-mode system [59–62], three tuning modes and one coupling mode, with parameters based on the multireference configuration interaction calculations of Woywood et al. [63]. To represent the remaining intramolecular modes of the molecule – the environment – Krempl et al. added 20 harmonic-oscillator modes with frequencies covering the range of the real pyrazine ground-state normal modes [51,64]. This environment consists in 20 tuning modes, with coupling constants equal in modulus but opposite in sign for the two electronic states. The parameters of the 4-mode system plus 20-mode environment are collected in Table 4. The Hamiltonian of the system is [51]

$$H_S = \sum_{s=10a,6a,1,9a} \frac{\omega_s}{2}(p_s^2 + x_s^2)\mathbf{1} + \begin{pmatrix} -\Delta + \sum\limits_{s=6a,1,9a} \kappa_s^{(1)} x_s & \lambda x_{10a} \\ \lambda x_{10a} & \Delta + \sum\limits_{s=6a,1,9a} \kappa_s^{(2)} x_s \end{pmatrix} \tag{34}$$

with the labelling of the modes following Ref. [65]. The Hamiltonian for the model $N_B = 20$ modes environment reads [51]

$$H_B = \sum_{i=1}^{N_B} \frac{\omega_i}{2}(p_i^2 + x_i^2)\mathbf{1} + \begin{pmatrix} \sum\limits_{i=1}^{N_B} \kappa_i^{(1)} x_i & 0 \\ 0 & \sum\limits_{i=1}^{N_B} \kappa_i^{(2)} x_i \end{pmatrix}. \tag{35}$$

Note that, here, we have $\kappa_i^{(1)} = -\kappa_i^{(2)}$ for all environmental modes, see Table 4. For this particular form of the Hamiltonian energy can flow to the environment only during a change of the diabatic state, *i.e.*, if $\lambda = 0$, system and environment are not coupled. This model system, or closely related ones, have been widely used to study the pyrazine as a benchmark case for the impact of an intramolecular environment, see, for instance, Refs. [51,64,50,14,66–68]. In Ref. [14], a full calculation treating all 24 modes with MCTDH is reported. This model has been also used to study, among others, the performance of the TDH approximation applied to an environment [50]. This is of interest

Table 4
Parameters of the original environment for the pyrazine example

Label	ω_i	$\kappa_i^{(1)}$	$\kappa_i^{(2)}$
ν_{10a}	0.0935	–	–
ν_{6a}	0.0740	−0.0964	0.1194
ν_1	0.1273	0.0470	0.2012
ν_{9a}	0.1568	0.1594	0.0484
1	0.0400	0.0069	−0.0069
2	0.0589	0.0112	−0.0112
3	0.0778	0.0102	−0.0102
4	0.0968	0.0188	−0.0188
5	0.1157	0.0261	−0.0261
6	0.1347	0.0308	−0.0308
7	0.1536	0.0210	−0.0210
8	0.1726	0.0265	−0.0265
9	0.1915	0.0196	−0.0196
10	0.2105	0.0281	−0.0281
11	0.2294	0.0284	−0.0284
12	0.2484	0.0361	−0.0361
13	0.2673	0.0560	−0.0560
14	0.2863	0.0433	−0.0433
15	0.3052	0.0625	−0.0625
16	0.3242	0.0717	−0.0717
15	0.3431	0.0782	−0.0782
18	0.3621	0.0780	−0.0780
19	0.3810	0.0269	−0.0269
20	0.4000	0.0306	−0.0306
$\Delta = 0.4617$		$\lambda = 0.1825$	

All values are in eV, and are taken from Krempl et al. [51]. The environmental modes (labelled by 1–20) are ordered in decreasing order of coupling strength.

for comparison with the present work. In fact, the conclusion of Ref. [50] is without appeal: TDH fails to correctly describe the dynamics provided by the environment. We have seen that this is also true for our former example when TDH is used to treat the original environment. Here, the particular form of the coupling to the system, purely electronic, along with the very strong nonadiabaticity of the problem, explain why the correlation between the modes play a key role, and, in turn, why the TDH method is not a good approximation for this problem. Indeed, the CI is located almost at the minimum of the upper surface and the spectrum is even stronger disturbed by the CI as compared to the butatriene example. Consequently we can view this example as a critical test for the TDH approximation.

We aim here at studying whether TDH can nevertheless give reasonable results when used on top of the effective-mode formalism or not. In addition, we shall investigate how the effective modes alone, without HRE, perform.

Interestingly, the model environmental Hamiltonian of Eq. (35) corresponds to a particular case of the effective-mode formalism. While we generally need *three* effective modes to construct each member of the hierarchy of effective Hamiltonians for a 2-state problem, like in the butatriene example, we need only *one* here. In Ref. [33], several special cases of the formalism are detailed, including this one, and we shall not give much details here. For the Hamiltonian in consideration, only a single-effective-mode can be identified, namely, $X_1 = \sum_{i=1}^{N_B} \kappa_i^{(1)} x_i$, because the interstate coupling of the environment is zero and the intrastate couplings are symmetric, $\kappa_i^{(1)} = -\kappa_i^{(2)}$. The procedure for constructing the higher members of the hierarchy and the corresponding residual environments is equivalent to the general case presented in Ref. [43] and exposed in Section 2.1.2. The first member of the hierarchy reads [33,36]

$$H_1 = \frac{\Omega_1}{2}(P_1^2 + X_1^2)\mathbf{1} + \begin{pmatrix} \bar{\kappa} X_1 & 0 \\ 0 & -\bar{\kappa} X_1 \end{pmatrix}$$

with $\bar{\kappa}$ given by Eq. (8). The higher members of the hierarchy are described accordingly by a single-effective-mode and are given by (for $m > 1$)

$$H_m = \frac{\Omega_m}{2}(P_m^2 + X_m^2)\mathbf{1} + d_{m-1,m}(P_{m-1}P_m + X_{m-1}X_m)\mathbf{1} \qquad (36)$$

and the mth residual environment (including $m = 1$) is given by

$$H_{rm} = \sum_{i=m+1}^{N_B} \frac{\Omega_i}{2}(P_i^2 + X_i^2)\mathbf{1} + \sum_{i=m+1}^{N_B} d_{m,i}(P_m P_i + X_m X_i)\mathbf{1}. \qquad (37)$$

We readily see that only H_1 has a contribution which is not diagonal in the electronic space and that the hierarchy reduces here to a sequential coupling of single-effective-modes. As before, the residual environments contain all the modes which are not included in the hierarchy. Note that the single-effective-mode Hamiltonian H_1 has already been used [36], and we are mainly concerned here with the hierarchy and the addition of the HRE. The parameters of the first four members of the hierarchy of effective Hamiltonians are presented in Table 5. Of course, the property regarding the moments discussed in Section 2.1.3 is preserved for this particular case: each time we add a single-effective-mode, two more moments are exactly reproduced. Finally, we mention that calculations based on *ab initio* data for all the 24 modes of the pyrazine molecule have been reported [15], but this study uses other parameters and implies a more involved Hamiltonian than the model discussed here.

3.3.1. Analysis of the effective-mode results

To illustrate the performance of the hierarchy of effective modes in this particular situation of the effective-mode formalism, we present the time-evolving diabatic populations of the upper, initially excited, electronic state, for the five following cases: 4-mode system alone and system

Table 5
Parameters of the first four single-mode effective Hamiltonians for the pyrazine example

Ω_1	0.3000	$\bar{\kappa}$	0.1860
Ω_2	0.2060	d_{12}	0.0710
Ω_3	0.2361	d_{23}	0.0876
Ω_4	0.2164	d_{34}	0.0900

All values are in eV.

plus one, two, three, and four effective modes. These cases correspond to the successive use of a zeroth-order hierarchy (no environment at all) to the 4th-order one which comprises four effective environmental modes here. The results are presented in Fig. 3. We see the important impact of the first effective mode, which suffices to correctly describe the fast initial decay of the excited state population. In particular, when the system's population slightly grows after a very short decay (between 2.5 and 5 fs), the use of a single-effective-mode suffices to correctly suppress this increase and the overall population decay is quite close to the exact one. A unique effective mode suffices to completely simulate the impact of the 24-mode environment on this very short-time-scale. In contrast, as we shall see in the next subsection, to include the five most strongly coupled modes of the original environment augmented by the TDH approximation for the 15 remaining modes is clearly not sufficient to correctly describe even the short-time dynamics.

To systematically illustrate the performance of the effective-mode formalism, let us look closer to the population dynamics between 7 and 30 fs, shown on enlarged scale in the inset of the figure. For the purpose of our discussion, we shall distinguish between time-scales for which the effective-mode results are very accurate, or numerically exact, and the larger time-scales where the results are no more numerically exact but are still reasonably accurate. In the inset, we see that the single-effective-mode result starts to deviate from the exact one around 7 fs. With a second EM, the result is numerically exact up to 12 fs. With 3 EMs, the time-scale is now 16 fs (although the differences up to 20 fs are very minor). With 4 EMs, the results are numerically exact up to 23 fs, but can almost not be distinguished from the exact one over the time-range considered in the inset. This exemplifies that, even in a particular case where only single-mode effective Hamiltonians are build, the use of more and more members of the hierarchy of effective Hamiltonians allows to reproduce, numerically exactly, the quantum dynamics of the entire system–environment complex.

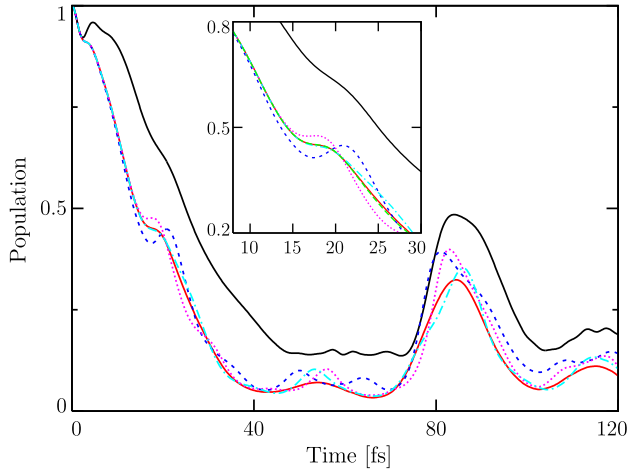

Fig. 3. Upper-state diabatic populations of the pyrazine model as a function of time. The (black) solid line above the other lines is the population for the 4-mode system alone. The (red) solid line is the 24-mode exact result. The (dark-blue) dashed line is the system plus 1 effective mode (EM) result; system plus 2 EM is in (pink) dotted, system plus 3 EM in (light-blue) dashed dotted, and system plus 4 EM (only in the inset) in (green) dashed. The inset zooms the population transfer from 7 to 30 fs, and illustrate how the addition of effective modes allows to accurately describe the dynamics over longer and longer time-scale when adding more effective modes, as predicted by the theory. Note that the 4 EM and exact result are almost identical. (For interpretation of the references in color in this figure legend, the reader is referred to the web version of this article.)

We turn now to the discussion of the large panel of Fig. 3. In this panel, the 4-EM result is not shown for clarity. We clearly see that the overall population dynamics is well reproduced using the various numbers of effective modes. When more effective modes are included, the results improve. With more effective modes, the results globally approach the exact one, even if it may not do so locally. We stress that, while the shape of the population dynamics is mainly given by the system, the increase in the population transfer due to the environment is large. For instance, at 15 fs, the population is 0.48 or 0.75 with or without the environment, respectively. The impact of the intramolecular environment is thus to enhance the population transfer. This can be explained by the lowering of the minimum of the intersection seam by the environmental modes, which also moves the location of this minimum closer to the coordinate origin [14]. The effective modes reproduce well the population transfer over the time-scale investigated.

3.3.2. Addition of the Hartree residual environment

For all the above-mentioned cases, we have additionally included the residual environment treated with TDH. While the population transfer is typically slightly improved, the addition of the HRE does not significantly and systematically improve all results for this example, and can even slightly deteriorate some effective-mode results. In fact, the HRE improves globally the description of the dynamics, over the whole time-range, by lowering for instance the too pronounced structures of the autocorrelation functions provided by the effective modes. However, some local oscillations of the autocorrelation functions may deviate more importantly with HRE than without, signaling the important impact of the correlation which is neglected at our level of approximation (this will be exemplified later in Fig. 5). In turn, while the global shape of the spectra are only slightly improved using HRE, some fine structures are described with a lower quality. In this critical case for TDH, to add an effective mode which subsumes all the correlations between the residual environmental modes on a given time-scale is clearly of higher quality than the treatment of the corresponding residual modes by TDH.

We want to show, however, that the use of the TDH approximation is nevertheless much more appropriate using the transformed versions of the Hamiltonian of the environment than the original one, even for this critical

model situation. We illustrate this by considering the following case, which was treated in Ref. [50] for this model environment of pyrazine. In the latter reference, calculations were done using the original Hamiltonian, Eq. (35), and treating different numbers of environmental modes "exactly", *i.e.*, with the proper multiconfiguration expansion, and the rest using Hartree products. This corresponds to the so-called independent-state Hartree (ISH) approximation already mentioned in Section 2.2.2. We shall compare the two different approaches, ISH and HRE. The ISH results are obtained by treating exactly the 4-mode system plus the five most strongly coupled environmental modes (the first five environmental modes in Table 4); the 15 remaining modes being treated with the ISH approximation. Following Ref. [50] we call this case 5MC + 15ISH (for 5 "multiconfiguration" and 15 ISH). We compare it with our result obtained by including the system plus 3 effective modes exactly, augmented by the 17-mode HRE.

We expose the differences between the ISH and HRE approximations by considering the (diabatic) population dynamics. Fig. 4 shows the populations for both cases, along with the system's population and the exact one. The 5MC + 15ISH result is not able to correctly describe the initial decay of the excited state population: the TDH approximation for the 15 modes is not sufficient even for the very short-time dynamics. In contrast, the 3EM + HRE result is of much better quality. For the initial decay up to 20 fs, the three effective modes do all the job, see Fig. 3. The HRE still improves the description of the population transfer and almost no difference with the exact result can be seen up to 40 fs. At later times the result remains of very good accuracy.

Fig. 5 shows the absolute value of the autocorrelation functions for the above cases when the upper electronic state is initially excited. The large panel contains the exact result along with the 3-EM one augmented or not by HRE. In the inset, the exact result is compared to the 5MC + 15ISH one. Note the different ordinate-scales between the large panel and the inset. Let us briefly discuss the large panel. The 3-EM result is indistinguishable from the exact one up to 20 fs and remains of very good quality over the entire time-range. In particular, not only the positions of the oscillations, but also the amplitudes, are very well reproduced. To add the HRE slightly improves the result roughly up to 40 fs. But then, the oscillations are slightly shifted compared to the exact or the effective-mode result and the intensities are now underestimated. While HRE may be thought of improving the effective-mode result, inspection of the real and imaginary part of the autocorrelation function (not shown) reveals that fine structures properly accounted for by the effective modes are disturbed by the HRE. Consequently, the HRE slightly deteriorates some fine structures of the spectra without significantly improving the global shape. However, these results remain of incomparably better quality than those obtained using TDH with the original environment. In

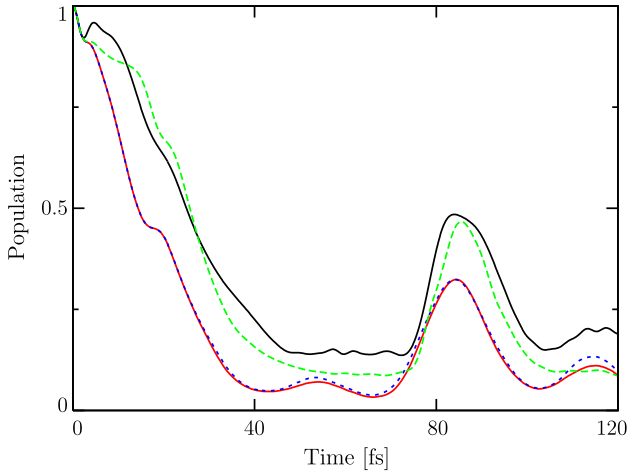

Fig. 4. Comparison of the population dynamics for the TDH approximation while using the original Hamiltonian or the hierarchy of effective Hamiltonians plus the residual environment. The pyrazine example is known to be critical for the TDH approximation [50]. The upper most (black) solid line is the result for the 4-mode system alone. The (red) solid line is the exact 24-mode result. The (green) dashed line is the result for the system's modes augmented by the five most important modes of the original environment, treated exactly, plus the 15 remaining modes treated with TDH (5MC + 15ISH, see text for details.) The (blue) short-dashed line is the result for the system plus 3 effective modes treated exactly plus the Hartree residual environment (HRE). (For interpretation of the references in color in this figure legend, the reader is referred to the web version of this article.)

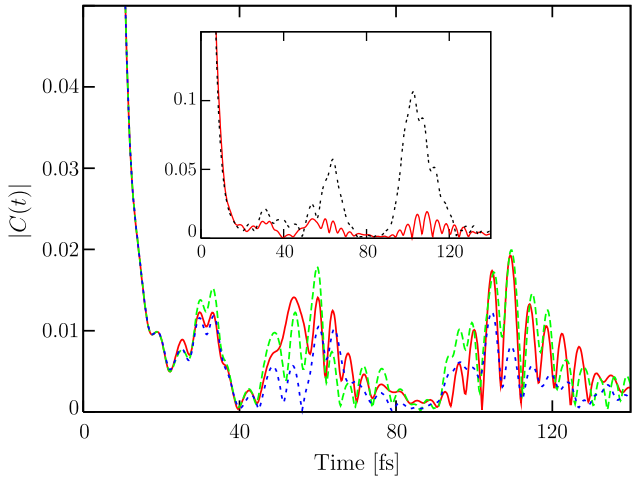

Fig. 5. Absolute value of the autocorrelation functions as a function of time for the pyrazine model. The (red) full line is the exact result. The (green) long-dashed line is the system plus 3 effective modes result. The (blue) short-dashed line is the result for the system plus 3 effective modes plus Hartree residual environment (HRE). The (black) dashed line are is result for the system's modes augmented by the five most important modes of the original environment, treated exactly, plus the 15 remaining modes treated with TDH (5MC + 15ISH, see text for details.) The large panel displays the exact result, and those for the system plus 3 effective modes augmented or not by the HRE. The inset shows the corresponding result for the 5MC + 15ISH case. Note that the ordinate-scale of the inset is enlarged by a factor of three. (For interpretation of the references in color in this figure legend, the reader is referred to the web version of this article.)

the inset of Fig. 5, we see that the 5MC + 15ISH result is simply wrong, in intensity as well as in the oscillating behavior. Recall that even more modes of the environment are treated exactly in the latter case (5 original modes against three effective modes).

4. Conclusions

In this paper, we have investigated the possibility to treat approximately the dynamics of the environment in macrosystems. The approach exploits the recently derived effective-mode formalism. This formalism, by the systematic construction of effective modes to represent the environment, allows one to reduce the dimensionality of the latter while including all the environmental effects for a given time-scale. This time-scale depends on the number of effective modes included. The two examples presented here show clearly that the inclusion of more and more effective modes allows to reproduce very accurately the dynamics of the entire macrosystem on longer and longer time-scales, as predicted by the theory [18,33,44]. Using a powerful wavepacket propagation technique, such as MCTDH, one can treat the quantum dynamics of the system modes augmented by some effective modes up to a total of 20–30 modes.

The residual modes – there may be many – are collected in a so-called residual environment. After the time-range of accuracy provided by the effective modes the residual environment has an impact on the dynamics. A full account of the residual environment is however out of reach, since it would correspond to treat all modes of the macrosystem. One can nevertheless use approximate dynamical schemes to describe the residual environment. Probably one of the simplest approximation, easily implemented when using MCTDH, consists in treating the residual environment by the TDH approximation, which we call Hartree residual environment (HRE).

The TDH approximation is known to fail to correctly reproduce the dynamics in conical-intersection situations. To test the performance of the approach used on top of the effective-mode formalism, we studied two examples comprising 22 and 24 modes in total to be able to compare to exact full-dimensional results. The first example corresponds to the general situation where three effective modes enter each effective Hamiltonian. For this example, the use of the HRE significantly improves the results provided by the system modes and a few effective modes. The action of the HRE is mainly to allow for the spreading of the wavepacket into the full-dimensional space, thus reducing the artificial recurrences which typically occurs after the time-range of accuracy of the effective modes is passed. We can then compute better resolved spectra while preserving their accuracy. Some local oscillations or structures of the autocorrelation functions of the effective-mode results may however be altered by the additional HRE, especially when correlations between the residual modes and the effective modes are very important.

This is exactly what happens in the second example dealing with pyrazine in a model environment. This example is known to be critical for the TDH approximation, which does not allow to correctly reproduce the dynamics. The effective-mode formalism performs very well by its owns. The population transfer is slightly improved when including the HRE but the autocorrelation functions and the resulting spectra are not and some fine details are even slightly deteriorated. For this special case correlations between the modes play the crucial role. These correlations are particularly strong for the pyrazine model but weaker for the butatriene one. The environmental modes cause mainly two effects, they firstly influence the location of the CI and secondly transfer vibrational energy from the system to the environment. The first process is a highly correlated one while the second process is more insensitive to an approximate description (or even neglect) of correlation. We speculate that for pyrazine, where the CI is close to the minimum of the upper diabatic surface and within the Frank–Condon zone, the first process is dominant, whereas for butatriene, where the CI is less easily accessible, the second process becomes dominant. This may explain the rather different behavior of the two systems on adding the HRE.

The correlations are fully included for the effective-mode part of the environment, but for the residual part the TDH approximation neglect them. Interestingly, this neglect amounts to almost kill the impact of the HRE for the pyrazine model, rather than to completely deteriorate the results. Consequently, one could say that, in the worst case, HRE does almost nothing regarding the quality of the effective mode results. In view of the small numerical cost of the TDH approximation, the HRE should be included. Of course, the addition of further effective modes, if possible without exceeding the numerical capabilities, is to be preferred – but then to add the corresponding HRE should also be possible. The dynamical properties of the effective-mode formalism indeed warrant an improvement of the results.

There is another advantage for including the HRE. Since it has no impact on the time-scale accurately reproduced by the effective modes alone, this time-scale can be obtained by inspecting when the HRE starts to contribute to the dynamics. In the absence of exact results to compare with, this provide a cheap and easy way to estimate the time-scale of accuracy.

The two examples show clearly the efficiency of the effective-mode formalism. While the results provided by the neglect of all the residual modes are very good over a given time-scale, the addition of the HRE significantly improves the results (butatriene) – or, at least, have almost no effect (pyrazine) – on the longer times. It is important to note that this is not the case if some selected modes of the original environment are treated correctly and the rest with TDH.

The effective-mode approach appears to be even more powerful in view of the possibility to additionally treat

the residual modes approximately. The main advantage of the TDH is the linear scaling of the numerical requirement with the number of residual modes, which renders its use feasible for truly large problems. Of course, other approximations may be used to treat the residual environment. One may think, in particular, to use Redfield theory [69], which is appropriate for so-called Markovian environments. The impact of the residual environment onto the system is mediated by the effective modes, and, if sufficiently many effective modes are included, the generally strongly non-Markovian behavior of the full environment at conical-intersection situations may turn into a more Markovian-like behavior of the residual part. This possibility could be studied, for instance, by adapting the approach used in Refs. [67,70] to the residual environment in the effective-mode formalism.

Acknowledgments

Fruitfull discussions with I. Burghardt are gratefully acknowledged. This work has been supported financially by the Deutsche Forschungsgemeinshaft (DFG). M.B. acknowledges support from the Graduiertenkolleg GRR 850/2 ''Molecular Modeling''.

References

[1] H. Köppel, W. Domcke, L.S. Cederbaum, Adv. Chem. Phys. 57 (1984) 59.
[2] J. Michl, V. Bonacić-Koutecký, Electronic Aspects of Organic Photochemistry, Wiley, 1990.
[3] D.R. Yarkony, Rev. Mod. Phys. 68 (1996) 985.
[4] W. Domcke, G. Stock, Adv. Chem. Phys. 100 (1997) 1.
[5] D.R. Yarkony, Acc. Chem. Res. 31 (1998) 511.
[6] M.A. Robb, M. Garavelli, M. Olivucci, F. Bernardi, in: K. Lipkowitz, D. Boyd (Eds.), Reviews in Computational Chemistry, vol. 15, Wiley, 2000, p. 87.
[7] M. Baer, G.D. Billing (Eds.), The Role of Degenerate States in Chemistry, Adv. Chem. Phys, vol. 24, Wiley, 2002.
[8] W. Domcke, D.R. Yarkony, H. Köppel (Eds.), Conical intersections: Electronic structure, Dynamics and Spectroscopy, World Sci., 2004.
[9] G.A. Worth, L.S. Cederbaum, Annu. Rev. Phys. Chem. 55 (2004) 127.
[10] S. Peruna, A.L. Sobolewski, W. Domcke, J. Am. Chem. Soc. 127 (2005) 6257.
[11] M. Abe, Y. Ohtsuki, Y. Fujimura, W. Domcke, in: T. Kobayashi et al. (Eds.), Ultrafast Phenomena, vol. XVI, Springer, 2005, p. 613.
[12] D.G. Truhlar, C.A. Mead, Phys. Rev. A 68 (2003) 032501.
[13] C.A. Mead, Rev. Mod. Phys. 64 (1992) 51.
[14] G.A. Worth, H.-D. Meyer, L.S. Cederbaum, J. Chem. Phys. 109 (1998) 3518.
[15] A. Raab, G.A. Worth, H.-D. Meyer, L.S. Cederbaum, J. Chem. Phys. 110 (1999) 936.
[16] A. Kühl, W. Domcke, J. Chem. Phys. 116 (2002) 263.
[17] I. Burghardt, L.S. Cederbaum, J.T. Hynes, Faraday Discuss. Chem. Soc. 127 (2004) 307.
[18] L.S. Cederbaum, E. Gindensperger, I. Burghardt, Phys. Rev. Lett. 94 (2005) 113003.
[19] H.D. Meyer, U. Manthe, L.S. Cederbaum, Chem. Phys. Lett. 165 (1990) 73.
[20] U. Manthe, H.-D. Meyer, L.S. Cederbaum, J. Chem. Phys. 97 (1992) 199.
[21] M.H. Beck, A. Jäckle, G.A. Worth, H.-D. Meyer, Phys. Rep. 324 (2000) 1.
[22] H.-D. Meyer, G.A. Worth, Theor. Chem. Acc. 109 (2003) 251.
[23] C. Cattarius, G.A. Worth, H.-D. Meyer, L.S. Cederbaum, J. Chem. Phys. 115 (2001) 2088.
[24] S. Mahapatra, G.A. Worth, H.-D. Meyer, L.S. Cederbaum, H. Köppel, J. Chem. Phys. 105 (2001) 5567.
[25] H. Köppel, M. Döscher, I. Bâldea, H.-D. Meyer, P.G. Szalay, J. Chem. Phys. 117 (2002) 2657.
[26] E.V. Gromov, A.B. Trofimov, N.M. Vitkovskaya, H. Köppel, J. Schirmer, H.-D. Meyer, L.S. Cederbaum, J. Chem. Phys. 121 (2004) 4585.
[27] A. Markmann, G.A. Worth, S. Mahapatra, H.-D. Meyer, H. Köppel, L.S. Cederbaum, J. Chem. Phys. 123 (2005) 204310.
[28] I. Bâldea, J. Franz, P.G. Szalay, H. Köppel, Chem. Phys. 329 (2006) 65.
[29] H. Wang, M. Thoss, J. Chem. Phys. 119 (2003) 1289.
[30] M. Thoss, H. Wang, Chem. Phys. 322 (2006) 210.
[31] G. Stock, M. Thoss, Adv. Chem. Phys. 131 (2005) 243.
[32] T.J. Martínez, Acc. Chem. Res. 39 (2006) 119.
[33] E. Gindensperger, I. Burghardt, L.S. Cederbaum, J. Chem. Phys. 124 (2006) 144103.
[34] I. Burghardt, E. Gindensperger, L.S. Cederbaum, Mol. Phys. 104 (2006) 1081.
[35] E. Gindensperger, I. Burghardt, L.S. Cederbaum, J. Chem. Phys. 124 (2006) 144104.
[36] I. Burghardt, J.T. Hynes, E. Gindensperger, L.S. Cederbaum, Phys. Scripta 73 (2006) C42.
[37] M.C.M. O'Brien, J. Phys. C 5 (1972) 2045.
[38] R. Englman, B. Halperin, Ann. Phys. 3 (1978) 453.
[39] M.C.M. O'Brien, S.N. Evangelou, J. Phys. C 13 (1980) 611.
[40] J.R. Fletcher, M.C.M. O'Brien, S.N. Evangelou, J. Phys. A 13 (1980) 2035.
[41] L.S. Cederbaum, E. Haller, W. Domcke, Solid State Commun. 35 (1980) 879.
[42] E. Haller, L.S. Cederbaum, W. Domcke, Mol. Phys. 41 (1980) 1291.
[43] E. Gindensperger, H. Köppel, L.S. Cederbaum, J. Chem. Phys. 126 (2007) 034107.
[44] E. Gindensperger, L.S. Cederbaum, J. Chem. Phys. 127 (2007) 124107.
[45] H. Tamura, E.R. Bittner, I. Burghardt, J. Chem. Phys. 126 (2007) 021103.
[46] H. Tamura, E.R. Bittner, I. Burghardt, J. Chem. Phys. 127 (2007) 034706.
[47] H. Tamura, A.G.S. Ramon, E.R. Bittner, I. Burghardt, arXiv:0707.2163v1 [cond-mat.soft] (2007).
[48] P.A. Dirac, Proc. Cambridge Philos. Soc. 26 (1930) 376.
[49] A.M. Lachlan, Mol. Phys. 8 (1964) 39.
[50] G. Worth, H.-D. Meyer, L.S. Cederbaum, J. Chem. Phys. 105 (1996) 4412.
[51] S. Krempl, M. Winterstetter, H. Plöhn, W. Domcke, J. Chem. Phys. 100 (1994) 926.
[52] N.G. van Kampen, Stochastic Processes in Physics and Chemistry, Elsevier Science Publishers B.V., 1992.
[53] U. Manthe, A.D. Hammerich, Chem. Phys. Lett. 211 (1993) 7.
[54] U. Manthe, H.-D. Meyer, L.S. Cederbaum, J. Chem. Phys. 97 (1992) 9062.
[55] V. Engel, Chem. Phys. Lett. 189 (1992) 76.
[56] A.J. Jerri, The Gibbs Phenomenon in Fourier Analysis, Splines and Wavelet Approximations, Kluwer, 1998.
[57] L.S. Cederbaum, W. Domcke, H. Köppel, W. von Niessen, Chem. Phys. 26 (1977) 169.
[58] G.A. Worth, M.H. Beck, A. Jäckle, H.-D. Meyer, The MCTDH Package, Version 8.2, (2000). H.-D. Meyer, Version 8.3 (2002), Version 8.4 (2007). <http://www.pci.uni-heidelberg.de/tc/usr/mctdh/>.
[59] R. Schneider, W. Domcke, Chem. Phys. Lett. 150 (1988) 235.
[60] R. Schneider, W. Domcke, H. Köppel, J. Chem. Phys. 92 (1990) 1045.

[61] G. Stock, W. Domcke, J. Chem. Phys. 93 (1990) 5496.
[62] R. Schneider, G. Stock, A.L. Sobolewsky, W. Domcke, J. Chem. Phys. 96 (1992) 5298.
[63] C. Woywood, W. Domcke, A.L. Sobolewsky, H.-J. Werner, J. Chem. Phys. 100 (1994) 1400.
[64] S. Krempl, M. Winterstetter, W. Domcke, J. Chem. Phys. 102 (1995) 926.
[65] K.K. Innes, I.G. Ross, W.R. Monaw, J. Mol. Spectrosc. 132 (1988) 492.
[66] B. Wolfseder, W. Domcke, Chem. Phys. Lett. 235 (1995) 370.
[67] A. Kühl, W. Domcke, J. Chem. Phys. 116 (2002) 263.
[68] I. Burghardt, H. Tamura, in: K.H. Hughes (Ed.), Dynamics of Open Quantum Systems, CCP6, 2006.
[69] A.G. Redfield, Adv. Magn. Reson. 1 (1965) 1.
[70] D. Egorova, W. Domcke, Chem. Phys. Lett. 384 (2004) 157.